separate, sequential reactions, each of which probably opens a binding site to permit one Na^+ to escape. Each charge component has well defined characteristics. The slowest appears to reflect strongly electrogenic (equivalent valence, $z \approx 1$; Fig. 2b) release of the first Na^+, through ~70% of the membrane field, in a reaction that is rate limited by the slow (~100 to 1,400 s^{-1}) major E_1-P ↔ P-E_2 conformational change, which itself seems relatively electroneutral; this slow component shows low sensitivity to $[Na]_o$ (Fig. 2b) but has strongly temperature-sensitive rates[5], revealing an enthalpic activation energy of ~80 kJ mol^{-1} (10–20 °C; not shown; see ref. 13). Like the slow component, the medium-speed (~6,000 to 20,000 s^{-1}) component also has a steeply voltage-dependent charge magnitude ($z \approx 1$; Fig. 4d), and a relaxation rate that increases with $[Na]_o$ at negative potentials and shows a high activation energy (~70 kJ mol^{-1}; not shown) and, hence, probably reflects the reaction that de-occludes the second Na^+. The fast component mirrors the time course of the distributed membrane capacitance transient and so must reflect charge transitions with rates $\geq 10^6$ s^{-1}, appropriate for rapid Na^+ release through an access channel, but still possibly rate limited by a minor conformational change that de-occludes the final Na^+; consistent with their high speed, these relaxations show little temperature sensitivity (not shown). In further contrast to the slow and medium-speed components, the fast charge movement has extremely weak voltage sensitivity (note simple scaling of the fast component amplitude with potential over a 160-mV range in Fig. 4c), and it is seen in virtual isolation at very low $[Na]_o$ ($\leq$25 mM; not shown), indicating that it may reflect release of the final Na^+ ion(s) from a relatively high-affinity site(s) on P-E_2 (see refs 8, 9, 12). Our failure to observe any comparably high-speed charge movement displaying the strong voltage sensitivity of the medium-speed and slow components, despite exploring a broad range of $[Na]_o$ and voltage, argues (see ref. 8) that there must be negligible steady-state occupancy of the narrow (high-field) access-channel conformation P-$E_2(Na_2)$·Na, which we propose (Fig. 4a) is ultimately responsible for those slower charge relaxations; this in turn implies that both rate constants leading away from that state (k_{-1} and k_2 in Fig. 4a) are relatively large.

The strictly sequential nature of the three charge components shown here indicates that the three Na^+ may be released from the Na^+/K^+ pump in a fixed order. Ordered occlusion/de-occlusion of two K^+ by kidney microsomal Na^+/K^+-ATPase[14] and sequential occlusion, translocation and release of the two Ca^{2+} ions transported by the sarcoplasmic reticulum Ca^{2+}-ATPase[15] have been detected using isotopes and rapid filtration techniques (time resolution ~10 ms), but the far higher time resolution and sensitivity of the electrical recording methods used here permit extraction of finer molecular kinetic detail[8,12,16]. Closer examination, using these methods, of the interactions of extracellular Na^+ ions with their binding sites within the Na^+/K^+ pump will now be required to discern the precise molecular rearrangements that surround these principal charge movements in the Na^+/K^+ transport cycle. □

Methods

Giant axons from the squid *Loligo pealei* were voltage clamped[17], internally dialysed and externally superfused at 20–22 °C with Cl^--free solutions[7,10] designed to restrict the pump to Na^+ de-occlusion/release steps (Fig. 1). Intracellular (in mM; pH adjusted with HEPES): 80 Na-HEPES, 57 *N*-methyl-D-glucamine(NMG)-HEPES, 50 glycine, 50 phenylpropyltriethylammonium-sulphate, 5 dithiothreitol, 2.5 1,2-bis(2-aminophenoxy)ethane-N,N,N′,N′-tetraacetic acid (BAPTA), 15 Mg-HEPES, 5 Tris-ATP, 5 phospho(enol)pyruvate tri-Na^+-salt and 5 phospho-L-arginine mono-Na^+-salt. Extracellular (in mM): 400 Na-isethionate, 75 Ca-sulphamate, 1 3,4-diaminopyridine, 2×10^{-4} tetrodotoxin, 5 Tris-HEPES and 0.05 EDTA (pH 7.7). Osmolality of all solutions was ~930 mOsmol kg^{-1}. To lower $[Na]_o$, Na-isethionate was replaced by tetramethylammonium-sulphamate or NMG-sulphamate. Voltage pulses were generated and currents recorded using a 16-bit PC44 A-D/D-A converter board (Innovative Technologies) with software developed in-house. Currents were filtered at 12.5–200 kHz, then sampled at 20 kHz–2 MHz. Current records were sometimes acquired after subtraction of appropriately amplified small current signals, obtained in a voltage range where pump-mediated charge movement tended towards saturation, to minimize currents from linear membrane capacitance. Pump current was determined as current sensitive to 100 μM H_2DTG[10].

Received 22 September; accepted 17 December 1999.

1. Post, R. L., Hegyvary, C. & Kume, S. Activation by adenosine triphosphate in the phosphorylation kinetics of sodium and potassium ion transport adenosine triphosphatase. *J. Biol. Chem.* **247,** 6350–6540 (1972).
2. Beaugé, L. A. & Glynn, I. M. Occlusion of K ions in the unphosphorylated sodium pump. *Nature* **280,** 510–512 (1979).
3. Garraham, P. J. & Glynn, I. M. The behaviour of the sodium pump in red cells in the absence of external potassium *J. Physiol.* **192,** 161–174 (1967).
4. Fendler, K., Grell, E., Haubs, M. & Bamberg, E. Pump currents generated by the purified Na^+K^+-ATPase from kidney on black lipid membranes. *EMBO J.* **4,** 3079–3085 (1985).
5. Nakao, M. & Gadsby, D. C. Voltage dependence of Na translocation by the Na/K pump. *Nature* **323,** 628–630 (1986).
6. Läiger. P. *Electrogenic Ion Pumps* (Sinauer, Sunderland, MA, 1991).
7. Gadsby, D. C., Rakowski, R. F. & De Weer, P. Extracellular access to the Na,K pump: pathway similar to ion channel. *Science* **260,** 100–103 (1993).
8. Hilgemann, D. W. Channel-like function of the Na,K pump probed at microsecond resolution in giant membrane patches. *Science* **263,** 1429–1432 (1994).
9. Heyse, S., Wuddel, I., Apell, H. J. & Sturmer, W. Partial reactions of the Na,K-ATPase: determination of rate constants. *J. Gen. Physiol.* **104,** 197–240 (1994).
10. Rakowski, R. F., Gadsby, D. C. & De Weer, P. Stoichiometry and voltage-dependence of the sodium pump in voltage-clamped, internally-dialyzed squid giant axon. *J. Gen. Physiol.* **93,** 903–941 (1989).
11. Läuger, P. & Apell, H. J. Transient behaviour of the Na^+/K^+-pump: microscopic analysis of nonstationary ion-translocation. *Biochim. Biophys. Acta* **944,** 451–464 (1988).
12. Wuddel, I. & Apell, H. J. Electrogenicity of the sodium transport pathway in the Na,K-ATPase probed by charge-pulse experiments. *Biophys. J.* **69,** 909–921 (1995).
13. Friedrich, T. & Nagel, G. Comparison of Na^+/K^+-ATPase pump currents activated by ATP concentration or voltage jumps. *Biophys. J.* **73,** 186–194 (1997).
14. Forbush, B. Rapid release of 42K or 86Rb from two distinct transport sites on the Na,K-pump in the presence of Pi or vanadate. *J. Biol. Chem.* **262,** 11116–11127 (1987).
15. Inesi, G. Characterization of partial reactions in the catalytic and transport cycle of sarcoplasmic reticulum ATPase. *J. Biol. Chem.* **262,** 16338–16342 (1987).
16. Lu, C.-C. *et al.* Memtrane transport mechanisms probed by capacitance measurements with megahertz voltage clamp. *Proc. Natl Acad. Sci. USA* **92,** 11220–11224 (1995).
17. Bezanilla, F., White, M. M. & Taylor, R. E. Gating currents associated with potassium channel activation. *Nature* **296,** 657–659 (1982).

Acknowledgements

This work was supported by grants from the NIH. M.H. was supported in part by the Grass Foundation, and J.W. held a HHMI Postdoctoral Research Fellowship for Physicians.

Correspondence and requests for materials should be addressed to D.C.G. (e-mail: gadsby@rockvax.rockefeller.edu), or to M.H. (e-mail: miguel_holmgren@hms.harvard.edu).

The 21-nucleotide *let-7* RNA regulates developmental timing in *Caenorhabditis elegans*

Brenda J. Reinhart*†, Frank J. Slack*†‡, Michael Basson‡§, Amy E. Pasquinelli*, Jill C. Bettinger‡#, Ann E. Rougvie#, H. Robert Horvitz§ & Gary Ruvkun*

** Department of Molecular Biology, Massachusetts General Hospital, and Department of Genetics, Harvard Medical School, Boston, Massachusetts 02114, USA*

§ Howard Hughes Medical Institute, Department of Biology, Massachusetts Institute of Technology, Cambridge, Massachusetts 02139, USA

 # Department of Genetics, Cell Biology and Development, University of Minnesota, St Paul, Minnesota 55108, USA

† These authors contributed equally to this work

The *C. elegans* heterochronic gene pathway consists of a cascade of regulatory genes that are temporally controlled to specify the timing of developmental events[1]. Mutations in heterochronic genes cause temporal transformations in cell fates in which stage-specific events are omitted or reiterated[2]. Here we show

‡ Present addresses: Axys Pharmaceuticals, South San Francisco, California 94080, USA (M.B.); Ernest Gallo Clinic and Research Center, UCSF, Emeryville, California 94608, USA (J.C.B.); Department of MCDB, Yale University, New Haven CT 06520, USA (F.J.S.).

that *let-7* is a heterochronic switch gene. Loss of *let-7* gene activity causes reiteration of larval cell fates during the adult stage, whereas increased *let-7* gene dosage causes precocious expression of adult fates during larval stages. *let-7* encodes a temporally regulated 21-nucleotide RNA that is complementary to elements in the 3′ untranslated regions of the heterochronic genes *lin-14*, *lin-28*, *lin-41*, *lin-42* and *daf-12*, indicating that expression of these genes may be directly controlled by *let-7*. A reporter gene bearing the *lin-41* 3′ untranslated region is temporally regulated in a *let-7*-dependent manner. A second regulatory RNA, *lin-4*, negatively regulates *lin-14* and *lin-28* through RNA–RNA interactions with their 3′ untranslated regions[3,4]. We propose that the sequential stage-specific expression of the *lin-4* and *let-7* regulatory RNAs triggers transitions in the complement of heterochronic regulatory proteins to coordinate developmental timing.

To identify new heterochronic genes, we carried out a genetic screen for mutations that suppress the synthetic sterile phenotype of a strain bearing the *lin-14(n179)* and *egl-35(n694)* mutations. We separated candidate suppressor mutations from the *lin-14* and *egl-35* mutations and examined each mutant for heterochronic defects. Out of 36 suppressor mutations isolated from animals carrying 44,000 mutagenized haploid genomes, the mutation *n2853* caused the strongest retarded heterochronic defects in a *lin14*(+) background (Fig. 1c; Table 1) and a temperature-sensitive adult lethal phenotype associated with vulval bursting. Another suppressor mutation, *mg279*, failed to complement *n2853* and caused a weak retarded phenotype (Table 1). We genetically mapped *n2853* and *mg279* and found that of the lethal mutations in the same region, *let-7(mn112)* (ref. 5) displayed heterochronic (Table 1) and lethal phenotypes (93% lethal, $n = 60$) nearly identical to that of *n2853*. *let-7(mn112)* is not temperature sensitive and failed to complement both *n2853* and *mg279*.

The first evidence of a *let-7* heterochronic defect is at the L4-to-adult moult. Hypodermal blast cells normally divide at each larval stage and at the adult stage exit the cell cycle, fuse with neighbouring hypodermal seam cells and generate cuticular alae[6] (Fig. 1a). In *let-7(n2853)* animals, the blast cell lineages were normal through the L3-to-L4 moult, but at the L4-to-adult moult, they reiterated larval patterns of cell division and failed to generate alae (Fig. 1a; Table 1). *let-7(n2853)* mutant animals reared at the permissive temperature underwent a supernumerary moult to a fifth larval stage, L5 (56%, $n = 26$). At the L5-to-adult moult, seam cells exited the cell cycle, fused with neighbouring seam cells, and produced alae (100%, $n = 10$ animals). The opposite phenotype resulted from over-expressing *let-7*. Increasing *let-7* gene dosage on a transgenic array caused hypodermal cells to precociously exit the cell cycle and terminally differentiate after the L3-to-L4 moult (83%, $n = 18$ animals). The opposite heterochronic phenotypes caused by reducing or increasing *let-7* activity indicate that *let-7* may function as a temporal switch between larval and adult fates.

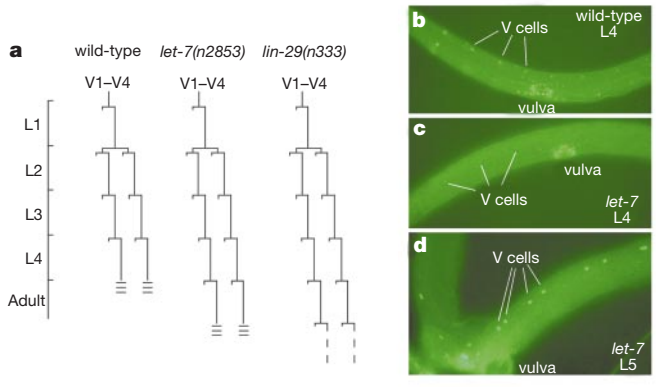

Figure 1 The *let-7* heterochronic phenotype. **a**, Lineage of the lateral hypodermal cells V1, V2, V3 and V4 in wild-type[6], *let-7(n2853)* and *lin-29(n333)* animals[2]. L3 and L4 stage V cell lineages are equivalent in hermaphrodites and cannot be distinguished. **b**, Wild-type L4 stage animal with LIN-29 expression in the lateral hypodermis and vulva. **c**, *let-7(n2853)* L4 stage animal with LIN-29 expression reduced in V cells but at normal levels in vulval cells. **d**, An L5 stage *let-7(n2853)* animal showing accumulation of LIN-29 at high levels one stage later than wild-type animals.

let-7 acts upstream of the heterochronic gene *lin-29*, a zinc-finger transcription factor that specifies adult-specific patterns of cell lineage and cell differentiation[2,7]. In wild-type animals, LIN-29 protein is expressed during the L4 and adult stages in hypodermal cells[8]. Consistent with the delay of adult differentiation by one stage in *let-7(n2853)* animals, LIN-29 expression in the hypodermis of L4 stage *let-7* animals was reduced relative to wild type, but expressed at normal levels at the L5 stage (Fig. 1b–d). Thus, *let-7* is necessary for the upregulation of LIN-29 expression in the hypodermis during the L4 stage, which in turn specifies adult cell fates.

The retarded alae phenotype caused by *let-7* mutations was partially suppressed by precocious mutations in the genes *lin-41*, *lin-42*, *lin-14* and *lin-28* (Table 1). For these epistasis experiments, we used the strong *let-7* allele *mn112*, which by molecular criteria completely eliminates gene function (see below). Mutations in *lin-41* and *lin-42* cause precocious expression of adult fates during late larval stages but do not affect L1 and L2 stage fates[9,10]. Thus, like *let-7* mutations, *lin-41* and *lin-42* mutations specifically affect late larval stage development and these three genes may function at about the same time during development. The *let-7* retarded heterochronic (Table 1) and lethal (F. J. Slack *et al.*, manuscript in preparation) phenotypes were partially suppressed by *lin-41* and *lin-42* mutations; conversely, the precocious alae phenotypes of *lin-41* and *lin-42* mutants were partially suppressed by a *let-7* mutation (Table 1). Although other interpretations are possible, these data are consistent with a model in which *lin-41* and *lin-42* are negatively regulated by *let-7*. Molecular analysis (see below) suggests that regulation by *let-7* may be direct.

Unlike *let-7* mutations, *lin-14* and *lin-28* mutations affect early larval development[2], suggesting that *let-7* functions later than *lin-14* and *lin-28*. For example, *lin-28*-null mutants delete L2 fates, but double mutant combinations with *let-7* did not suppress this early defect (Table 1). However, the reiteration of larval fates caused by the *let-7*-null mutation was partially suppressed by the precocious expression of adult fates caused by *lin-28* or *lin-14* null mutations

Table 1 Phenotype of *let-7* mutants and interactions with other heterochronic mutants

	Percentage of animals with adult lateral alae*			
Strain	L3 moult		L4 moult	
Wild-type (N2)	0	(25)	100	(25)
let-7(mn112) unc-3(e151)	0	(20)	0	(20)
let-7(n2853) 15 °C	0	(20)	0	(20)
let-7(n2853) 25 °C	0	(30)	0	(20)
let-7(mg279)	0	(20)	100†	(24)
lin-41(ma104)	54†	(48)	100	(45)
lin-41(ma104); let-7(mn112) unc-3(e151)	0	(18)	70	(20)
lin-42(n1089)	90†	(72)	100	(58)
lin-42(n1089); let-7(mn112) unc-3(e151)	13	(66)	31	(86)
lin-14(n536 n540)	100	(25)	100	(25)
lin-14(n536 n540) let-7(mn112) unc-3(e151)	44†	(36)	70	(46)
lin-14(n179) 25 °C	100	(38)	100	(28)
lin-14(n179) let-7(mn112) unc-3(e151) 25 °C	18	(32)	30	(129)
lin-28(n719)	100	(20)	100	(20)
lin-28(n719); let-7(mn112); unc-3(e151)‡	7†	(60)	17†	(58)
lin-4(e912)	0	(20)	0	(20)
lin-4(e912); let-7(mn112) unc-3(e151)	0	(20)	0	(40)

All strains were grown at 20° unless otherwise indicated.
* The number of animals is given in parentheses.
† Some animals had patches of alae rather than continuous alae, indicating a mix of larval fates for some V cells and adult fates for others. Percentage of animals with patches: 29% of *let-7(mg279)* adults; 25% of *lin-41(ma104)* L4s; 28% of *lin-42(n1089)* L4s; 33% of *lin-14(n536n540) let-7(mn112) unc-3(e151)* L4s; 7% of *lin-28(n719); let-7(mn112) unc-3(e151)* L4s; and 17% of lin-28 (n719); *let-7(mn112) unc-3(e151)* adults.
‡ In *lin-28; let-7* animals, the postdeirid cells derived from the V5 blast cell during the L2 stage were absent in L4-stage animals ($n = 5$), suggesting that the deletion of V cell L2 fates caused by the *lin-28(n719)* null mutation was not suppressed.

(Table 1). This suggests that the early developmental effects of *lin-14* and *lin-28* affect *let-7* function at late larval stages. Because the *let-7* null mutant phenotype is not epistatic to *lin-14* and *lin-28* null mutations, *let-7* is not the only output of these earlier acting genes. Molecular analysis of *let-7* (see below) indicates that direct regulation of *lin-14* and *lin-28* by *let-7* is also possible.

By a combination of transgene complementation, RNA expression analysis and mutant allele sequencing, we established that *let-7* encodes an untranslated RNA. This analysis mapped *let-7* to a 2.5-kilobase (kb) region of cosmid C05G5 that fully complemented *let-7(mn112)* (Fig. 2a). The three *let-7* mutations cluster in a 200-base pair (bp) segment: *let-7(mn112)* and *let-7(mg279)* are 190-bp and 27-bp deletions, respectively; and *let-7(n2853)* is a substitution within four bases of *mn112* (Fig. 2b). No protein-coding genes are predicted in the region, and no messenger RNAs were detected by probing complementary DNA libraries or by northern analysis for RNAs larger than 100 nucleotides (data not shown).

Because these studies did not identify a conventional *let-7* gene product, we used evolutionary conservation of *let-7* DNA sequences between two species of *Caenorhabditis* separated by 40 million years[11] to reveal probable functional sequences[12]. A 2.3-kb genomic DNA fragment from *Caenorhabditis briggsae* complemented *let-7(mn112)*, showing that *let-7* function is conserved between the two species (data not shown). Comparison of *C. elegans* and *C. briggsae* *let-7* identified regions of high sequence identity (Fig. 2b). Notably, a 26-bp region flanking the *let-7(n2853)* point mutation is conserved.

We detected a 21-nucleotide RNA transcript by northern analysis of small RNAs probed with an oligonucleotide from the conserved region flanking the *let-7* mutations (Fig. 3a). This 21-nucleotide RNA was undetectable in the *let-7(mn112)*-deletion mutant and reduced in abundance in the *let-7(n2853)* mutant. S1 nuclease analysis established the *let-7* RNA sequence as UGAGGUAGUAG-GUUGUAUAGU (Fig. 3b, c). *let-7(mn112)* deletes the first base of the transcript and 189 bases of upstream sequence, consistent with the observation that the transcript is not produced in this mutant and indicating that *let-7(mn112)* may be a null mutant. *let-7(n2853)* alters the fifth nucleotide of the *let-7* transcript. *let-7(mg279)* deletes a possible transcriptional regulatory domain upstream of the *let-7* transcript (Fig. 2b). The *let-7* RNA is unlikely to be translated: no AUG is present in any potential reading frame and the exact *C. elegans* and *C. briggsae* sequence conservation is inconsistent with the expected variation in degenerate codon positions of a translated product. The 21-nucleotide *let-7* RNA is not likely to be spliced onto a single larger transcript, because the size matches the transcript detected by northern analysis and no other transcripts were detected using the 2.5-kb rescuing fragment as a probe. One conserved region, 400bp away, contains a methionine codon (Fig. 2b), but site-directed mutagenesis of this codon in the *C. elegans* 2.5-kb rescuing fragment did not disrupt *let-7* function (data not shown). The close correspondence of the *let-7* mutations with this small RNA product, its conservation in *C. briggsae*, and the lack of open reading frames strongly support our conclusion that *let-7* functions as an RNA molecule.

let-7 expression is temporally regulated: *let-7* RNA was not detected at embryonic, L1 or L2 stages; low-level expression was

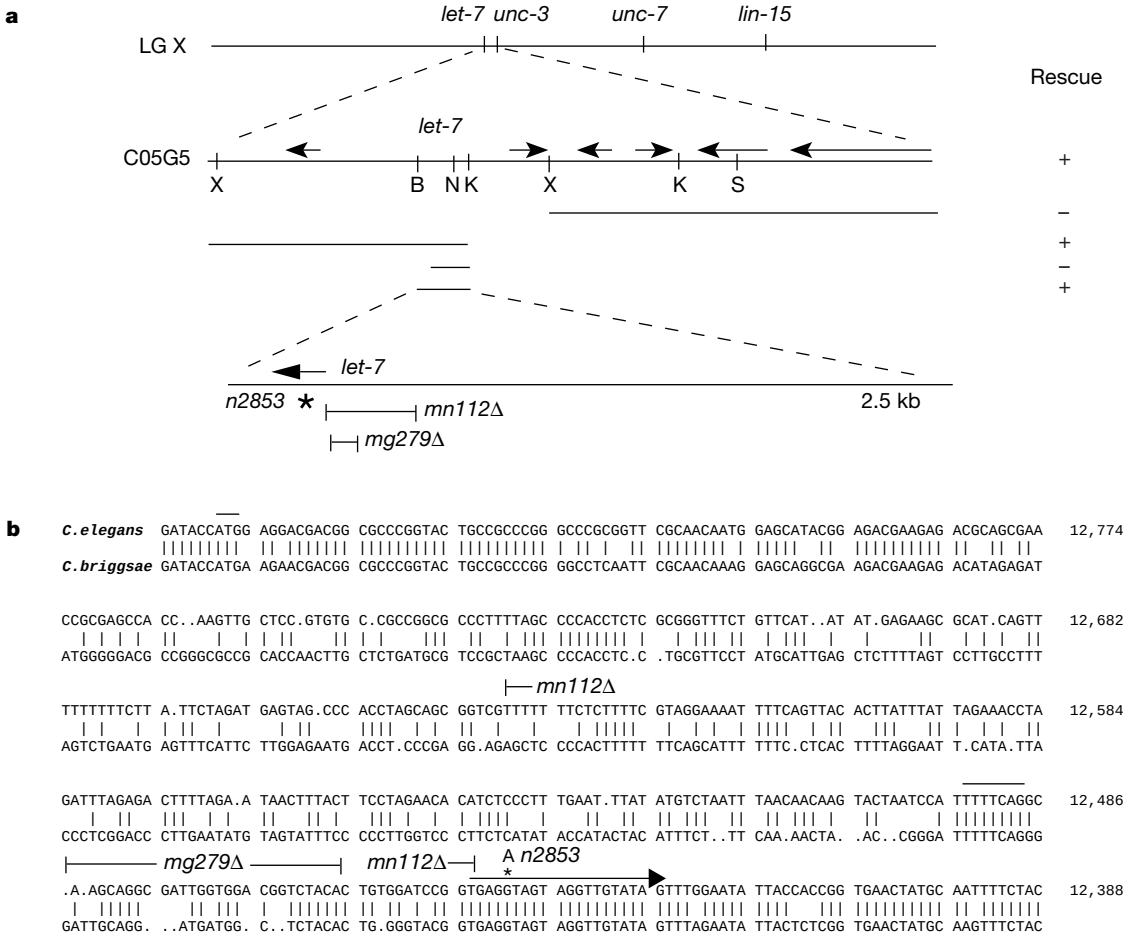

Figure 2 The *let-7* gene sequence. **a**, Transgenic rescue. +, more than 90% rescue in multiple lines; –, no rescue. Arrows above C05G5 indicate predicted genes. **b**, Sequence comparison of *let-7* from *C. elegans* and *C. briggsae*. The 2.5-kb genomic fragment that fully rescues *let-7(mn112)* corresponds to nucleotide positions 14,208–11,749 of cosmid C05G5. The 21-nucleotide *let-7* transcript is indicated by an arrow. A truncation of the 2.5-kb fragment (to 12,446) deleting this transcript no longer rescues *let-7(mn112)*. The ATG at 12,857 and a 3′ splice consensus TTTTCAG of a non-conserved open reading frame at 12,494 are indicated by bars.

detected at the early L3 stage; and high-level expression was detected at the early L4 and adult stages (Fig. 3d). This expression profile is consistent with the *let-7* mutant phenotype, which affects development specifically in late larval and adult stages. Expression of *let-7* in late larval stages also coincides with the critical period for *let-7* function in viability as determined by temperature-shift experiments (Fig. 3e).

Given the genetic interactions observed between *let-7* and other heterochronic genes (Table 1) and the precedent for direct interaction between the *lin-4* regulatory RNA and genes in the heterochronic pathway, we searched for complementary regions between the *let-7* RNA and the mRNAs of these heterochronic genes. Five heterochronic genes contain sequences complementary to *let-7* in their experimentally determined (*lin-14*[13], *lin-28*[4] and *lin-41* (F. J. Slack *et al.*, manuscript in preparation)) or predicted (*daf-12*[14] and *lin-42*[15]) 3′ untranslated regions (UTRs) but not elsewhere in these mRNAs (Fig. 4a). The *let-7(n2853)* mutation would affect all predicted duplexes. The sequences of the *lin-28* element and three of the four *lin-14* elements are conserved in other Caenorhabditae.

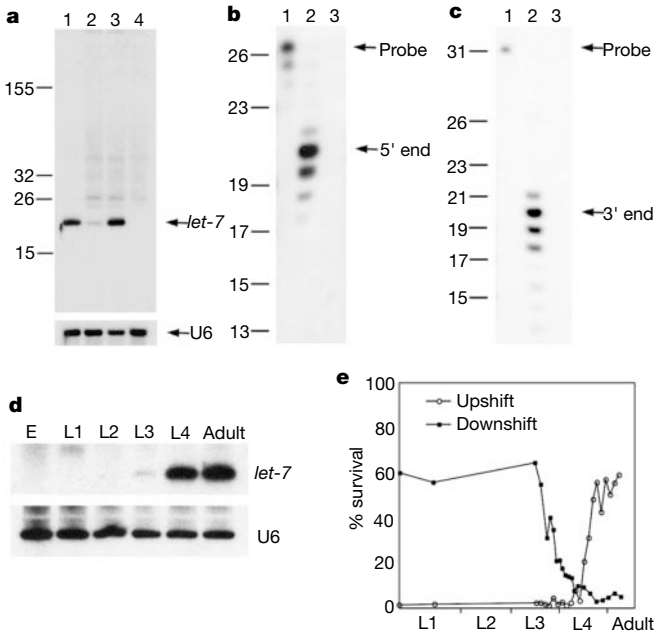

Figure 3 The 21-nucleotide *let-7* RNA. **a**, Northern blot of total RNA from mixed stage wild-type (lane 1), *let-7(n2853)* (lane 2), *lin-28(n719)* (lane 3) and *lin-28(n719); let-7(mn112) unc-3(e151)* animals (lane 4) probed with p249N. **b**, **c**, S1 nuclease transcript mapping. **b**, 5′ probe p263 undigested (lane 1), and digested after hybridization to wild-type RNA (lane 2) or tRNA (lane 3). **c**, 3′ probe p267 undigested (lane 1), and digested after hybridization to wild-type RNA (lane 2) or tRNA (lane 3). Sizing ±1 nucleotide. **d**, Northern blot of wild-type RNA from the first 3 hours of each developmental stage. **e**, Temperature-sensitive period of *let-7(n2853)* viability.

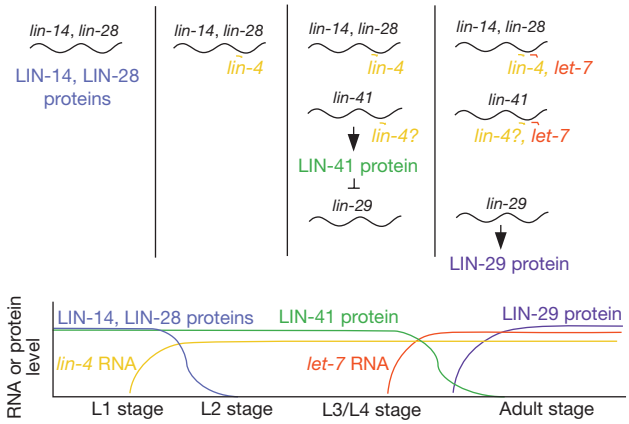

Figure 5 A model for the successive regulation of heterochronic gene activities by the *lin-4* and *let-7* RNAs. LIN-14 and LIN-28 expression levels are decreased by *lin-4* RNA expression at the end of the first larval stage to allow progression to late larval stages. In late larval stages, the expression of LIN-41 and other genes may be similarly downregulated by the *let-7* RNA, relieving their repression of LIN-29 protein expression and allowing progression to the adult stage. Because the *lin-29* mRNA does not contain sites complementary to the *let-7* RNA, *lin-29* is not likely to be a direct target of *let-7*.

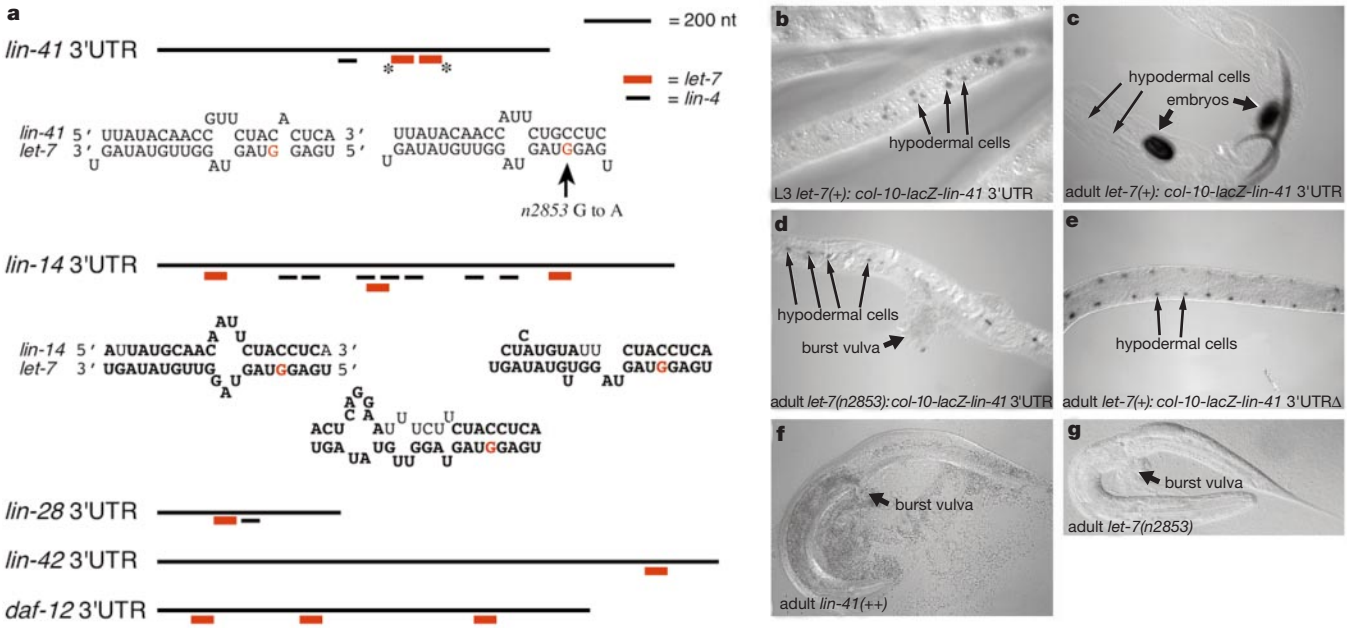

Figure 4 *let-7* regulation of heterochronic genes. **a**, *let-7* complementary sites in heterochronic genes. Bases shown in bold are conserved in genes with known *C. briggsae* homologues. **b**–**e**, *let-7* regulation of *lin-41*. A *col-10/lacZ/lin-41* 3′ UTR reporter gene was expressed in hypodermal cells of *let-7(+)* L3 larvae (**b**), downregulated in *let-7(+)* adults (**c**), but expressed at high levels in *let-7(n2853)* adults (**d**); deletion of the *let-7* complementary sites in this reporter gene 3′ UTR (between asterisks in **a** allows expression in *let-7*(+) adults (**e**). **f**, **g**, *lin-41* is a major *let-7* target. High dosage of *lin-41*(+) in wild-type (**f**) caused a bursting phenotype similar to *let-7(N2853)* (**g**).

The segments complementary to *let-7* are located adjacent to or overlapping segments complementary to the *lin-4* regulatory RNA in the *lin-14*, *lin-28* and *lin-41* 3′ UTRs, suggesting that the two RNAs may both regulate the expression of these target genes. The *lin-29* 3′ UTR lacks a *let-7* complementary region, suggesting that the regulatory interaction between *let-7* and *lin-29* is indirect. On the basis of the 36% G+C content of *C. elegans* DNA and the length of each 3′ UTR, the probabilities of detecting the blocks of exact sequence complementarity to *let-7* by chance are 10^{-6} for *lin-14*, 5×10^{-5} for *lin-41*, 10^{-4} for *daf-12*, 10^{-3} for *lin-42* and 0.05 for *lin-28*. Clusters of elements were not detected in a randomly chosen set of 3′ UTRs (1 isolated element in 26 3′ UTRs).

Genetic analysis indicates that it may be dysregulation of *lin-41* in a *let-7* mutant that causes most of the lethal and heterochronic phenotypes (Fig. 4b–g): increasing the gene dose of *lin-41* causes the distinctive vulval bursting (Fig. 4f, g) and heterochronic phenotypes (F. J. Slack *et al.*, manuscript in preparation) of a *let-7* loss-of-function mutant; loss-of-function mutations in *lin-41* constitute the strongest class of mutations that suppress the *let-7* lethal mutant (F. J. Slack *et al.*, manuscript in preparation); and *lin-41* acts in late larval development[9] and is downregulated at the time of *let-7* expression.

The sites that are complementary to the *let-7* RNA in the *lin-41* 3′ UTR mediate *let-7*-dependent temporal downregulation of a *lac-Z* reporter gene. A reporter bearing the *lin-41* 3′ UTR was expressed in larval stage but not adult wild-type animals (Fig. 4b, c), similar to the temporal regulation of the *lin-41* gene itself (F. J. Slack *et al.*, manuscript in preparation), whereas a control reporter bearing the *unc-54* 3′ UTR was expressed at all stages[16]. The *lacZ/lin-41* 3′ UTR fusion gene was expressed in 79% ($n = 14$) of *let-7 (n2853)* adult animals (Fig. 4d) but only 19% ($n = 21$) of wild-type adults. Deletion of the *let-7* complementary sites from the *lin-41* 3′ UTR resulted in expression of the reporter gene in 77% of wild-type adults ($n = 30$) (Fig. 4e). These data strongly suggest that the *let-7* complementary sites in the *lin-41* 3′ UTR bind to the *let-7* regulatory RNA during the L4 and adult stages to mediate downregulation of *lin-41* gene activity. The functions of *let-7* complementary sites in the 3′ UTRS of *lin-42* or *daf-12* have not been assessed.

The *let-7* complementary sequences in *lin-14* and *lin-28* are more difficult to rationalize, because *lin-14* and *lin-28* function earlier in development than does *let-7* and the expression of the LIN-14 and LIN-28 proteins is downregulated by the *lin-4* regulatory RNA[3,4,16] before the onset of *let-7* RNA expression. In fact, no major alterations in the timing or levels of LIN-14 (data not shown) or *lin-28*::GFP (green fluorescent protein)[4] expression (V. Ambros, personal communication) were observed in *let-7* mutant animals, suggesting that either *let-7* does not regulate the expression of these genes or that *let-7* regulation of these genes is more subtle than its regulation of *lin-41*.

Two regulatory RNAs are now known to function in the heterochronic pathway. Expression of *lin-4* RNA before the second larval moult[17] negatively regulates LIN-14 and LIN-28 levels to signal a transition from early to later larval patterns of cell lineage and differentiation. Expression of the *let-7* RNA during the L3 and later stages negatively regulates *lin-41* and perhaps other gene activities to signal the transition to the adult stage. Even though the *lin-4* and *let-7* RNAs are not homologous, the mechanism by which they regulate the expression of their target genes could be related. These heterochronic small RNA genes may constitute elements of a cascade of stage-specific regulatory RNAs that control the temporal sequence of events in *C. elegans* development (Fig. 5). □

Methods

Screen for retarded heterochronic genes

egl-35(n694ts)[18] in combination with the temperature-sensitive *lin-14(n179ts)* mutation causes a sterile phenotype. To isolate suppressor mutations, we picked fertile progeny from mutagenized *egl-35(n694ts)*; *lin-14(n179ts)* animals. See http://xanadu.mgh.harvard.edu/ruvkunweb/papers.html for details concerning the genetic screen by which we identified *let-7* and the genetic mapping of *let-7*. To examine retarded heterochronic development, we observed *let-7(n2853)* animals using Nomarski optics and counted V cells and descendants at mid L1 ($n = 12$ animals), early L2 ($n = 5$), mid L2 ($n = 33$), mid L3 ($n = 29$), mid L4 ($n = 30$) and early adult ($n = 12$) stages. For the temperature-sensitive period analysis, synchronized *let-7(n2853)* animals were either upshifted or downshifted between 15° and 25° at the indicated time and scored for viability 1 day after the L4 moult.

Transgenics

For rescue experiments, genomic clones and linear PCR fragments were microinjected into *let-7* mutant animals at 2–5 ng μl^{-1} with a *goa-1*::GFP fusion gene at 70–85 ng μl^{-1} as a co-injection marker[19]. Transgenes with no rescuing activity (–) were maintained as balanced lines. We identified a *C. briggsae let-7* genomic λ clone by hybridization to a *C. elegans let-7* probe. A 2.3-kb *C. briggsae* region (GenBank accession number AF210771) was amplified using PCR from the λ clone and tested for rescuing activity by injection at 5 ng μl^{-1}. For *let-7* and *lin-41* overexpression experiments, either 10 ng μl^{-1} of the 2.5-kb rescuing region of *let-7* or 5 ng μl^{-1} of the *lin-41* containing cosmid C12C8 was co-injected with *goa-1*::GFP into wild-type animals. The 1148-bp *lin-41* 3′ UTR was amplified using PCR and cloned 3′ to the *col-10/lacZ* reporter gene[16]. The same transgene array that was analysed in a *let-7*(+) genetic background was crossed into the *let-7(n2853)* genetic background. To delete the *let-7* complementary sites, a deletion of 85 bp (15,565–15,650 in cosmid C12C8) in the 1148-bp *lin-41* 3′ UTR region was constructed by PCR and the 1063-bp fragment was similarly cloned 3′ to the *col-10/lacZ* fusion gene. Reporter genes were co-injected with a *goa-1*::GFP reporter and only GFP^+ transgenic animals were picked for fixation and staining.

RNA analysis

RNA was isolated from *lin-28(n719); let-7(mn112) unc-3(e151)* mutants because *lin-28(n719)* suppressed the lethality of *let-7(mn112)*. Total RNA preparation, northern analysis, and S1 nuclease protection assays were done as described[19,20]. 5′ end-labelled probes were p249N, 5′-AACTATACAACCTACTACCTCACCGGATCC-3′, p263, 5′-CTATACAACCTACTACCTCACCGGAT-3′, pU6, 5′-GCAGGGGCCATGC-TAATCTTCTCTGTATTG-3′. For 3′ end mapping p267, 5′-TAATATTCCAAACTATA-CAACCTACTACCT-3′, was annealed to p268, 5′-TGAGGTAGTAGGTTGTATAG-3′, and labelled at the 3′ end with Klenow and [α-^{32}P] dGTP. Potential RNA–RNA duplexes were identified by a combination of manual searching and computer analysis using the FOLDRNA program of the GCG software package[21].

Received 7 October; accepted 6 December 1999.

1. Ambros, V. A hierarchy of regulatory genes controls a larva-to-adult developmental switch in *C. elegans*. *Cell* **57,** 49–59 (1989).
2. Ambros, V. & Horvitz, H. R. Heterochronic mutants of the nematode *Caenorhabditis elegans*. *Science* **226,** 409–416 (1984).
3. Lee, R. C., Feinbaum, R. L. & Ambros, V. The *C. elegans* heterochronic gene *lin-4* encodes small RNAs with antisense complementarity to *lin-14*. *Cell* **75,** 843–854 (1993).
4. Moss, E. G., Lee, R. C. & Ambros, V. The cold shock domain protein LIN-28 controls developmental timing in *C. elegans* and is regulated by the *lin-4* RNA. *Cell* **88,** 637–646 (1997).
5. Meneely, P. M. & Herman, R. K. Lethals, steriles, and deficiencies in a region of the X chromosome of *Caenorhabditis elegans*. *Genetics* **92,** 99–115 (1979).
6. Sulston, J. E. & Horvitz, H. R. Post-embryonic cell lineages of the nematode *Caenorhabditis elegans*. *Dev. Biol* **56,** 110–156 (1977).
7. Rougvie, A. E. & Ambros, V. The heterochronic gene *lin-29* encodes a zinc finger protein that controls a terminal differentiation event in *Caenorhabditis elegans*. *Development* **121,** 2491–2500 (1995).
8. Bettinger, J. C., Lee, K. & Rougvie, A. E. Stage-specific accumulation of the terminal differentiation factor LIN-29 during *Caenorhabditis elegans* development. *Development* **122,** 2517–2527 (1996).
9. Liu, Z. *Genetic Control of Stage-Specific Developmental Events in C. elegans.* Thesis, Harvard Univ. (1990).
10. Abrahante, J. E., Miller, E. A. & Rougvie, A. E. Identification of heterochronic mutants in *Caenorhabditis elegans*: temporal misexpression of a collagen::green fluorescent protein fusion gene. *Genetics* **149,** 1335–1351 (1998).
11. Kennedy, B. P. *et al.* The gut esterase gene (*ges-1*) from the nematodes *Caenorhabditis elegans* and *Caenorhabditis briggsae*. *J. Mol. Biol.* **229,** 890–908 (1993).
12. Zucker-Sparison, E. & Blumenthal, T. Potential regulatory elements of nematode vitellogenin genes revealed by interspecies sequence comparison. *J. Mol. Evol.* **28,** 487–496 (1989).
13. Wightman, B. *et al.* Negative regulatory sequences in the *lin-14* 3′-untranslated region are necessary to generate a temporal switch during *Caenorhabditis elegans* development. *Genes. Dev.* **5,** 1813–1824 (1991).
14. Yeh, W. H. *Genes Acting Late in the Signaling Pathway for Caenorhabditis elegans* Dauer Larval Development. Ph.D. Thesis. University of Missouri, Columbia, MO (1991).
15. Jeon, M., Gardner, H. F., Miller, E. A., Deshler, J. & Rougvie, A. E. Similarity of the *C. elegans* developmental timing protein LIN-42 to circadian rhythm proteins. *Science* **286,** 1141–1146 (1999).
16. Wightman, B., Ha, I. & Ruvkun, G. Posttranscriptional regulation of the heterochronic gene *lin-14* by *lin-4* mediates temporal pattern formation in *C. elegans*. *Cell* **75,** 855–862 (1993).
17. Feinbaum, R. & Ambros, V. The timing of *lin-4* RNA accumulation controls the timing of postembryonic developmental events in *C. elegans*. *Dev. Biol.* **210,** 87–95 (1999).
18. Trent, C., Tsung, N. & Horvitz, H. R. Egg-laying defective mutants of the nematode *Caenorhabditis elegans*. *Genetics* **104,** 619–647 (1983).
19. Segalat, L., Elkes, D. A. & Kaplan, J. M. Modulation of serotonin-controlled behaviors by G_o in *Caenorhabditis elegans*. *Science* **267,** 1648–1651 (1995).
20. Ausubel, F. M. *et al. Current Protocols in Molecular Biology* (John Wiley & Sons, New York, 1995).
21. Devereux, J., Haeberli, P. & Smithies, O. A comprehensive set of sequence analysis programs for the VAX. *Nucleic Acids Res.* **12,** 387–395 (1984).

Acknowledgements

We thank the *C. elegans* Genome Sequencing Consortium for sequence data, A. Coulson and the Sanger Centre for cosmids, the *Caenorhabditis* Genetics Center and V. Ambros for providing strains and sharing unpublished results. We thank R. Feinbaum for advice concerning experimental procedures and Y. Liu and P. Delerme for technical assistance. This work was supported by NIH grants to G.R., H.R.H. and A.R., and an NIH postdoctoral fellowship to F.S. H.R.H. is an Investigator of the Howard Hughes Medical Institute.

Correspondence and requests for materials should be addressed to G.R.

Pgh1 modulates sensitivity and resistance to multiple antimalarials in *Plasmodium falciparum*

Michael B. Reed*, Kevin J. Saliba†, Sonia R. Caruana*, Kiaran Kirk† & Alan F. Cowman*

** The Walter and Eliza Hall Institute of Medical Research, Melbourne, Victoria 3050, Australia*
† Division of Biochemistry and Molecular Biology, Faculty of Science, Australian National University, Canberra 0200, Australia

Throughout the latter half of this century, the development and spread of resistance to most front-line antimalarial compounds used in the prevention and treatment of the most severe form of human malaria has given cause for grave clinical concern. Polymorphisms in pfmdr1, the gene encoding the P-glycoprotein homologue 1 (Pgh1) protein of *Plasmodium falciparum*, have been linked to chloroquine resistance[1]; Pgh1 has also been implicated in resistance to mefloquine and halofantrine[2–5]. However, conclusive evidence of a direct causal association between pfmdr1 and resistance to these antimalarials has remained elusive, and a single genetic cross has suggested that Pgh1 is not involved in resistance to chloroquine and mefloquine[6]. Here we provide direct proof that mutations in Pgh1 can confer resistance to mefloquine, quinine and halofantrine. The same mutations influence parasite resistance towards chloroquine in a strain-specific manner and the level of sensitivity to the structurally unrelated compound, artemisinin. This has important implications for the development and efficacy of future antimalarial agents.

Two alleles of the *pfmdr1* gene identified in field isolates of *P. falciparum* are linked with chloroquine resistance (CQR). One of these, the '7G8 allele', encodes four amino-acid substitutions with respect to the chloroquine-sensitive (CQS) 'D10 allele': Tyr 184 to Phe 184; Ser 1034 to Cys 1034; Asn 1042 to Asp 1042; and Asp 1246 to Tyr 1246 (refs 1–7). To examine the role of the last three mutations of Pgh1 in controlling parasite sensitivity and resistance to antimalarials, we constructed plasmids for *P. falciparum* transformation and allelic exchange at the endogenous *pfmdr1* locus[8].

Plasmid pHC1-mdr^{7G8} replaced the *pfmdr1* gene in CQS D10 parasites such that the protein carried the mutations Cys 1034, Asp 1042 and Tyr 1246. Plasmid pHC1-mdr^{D10} (Fig. 1a) served as a transfection control and resulted in retention of the amino acids Ser 1034, Asn 1042 and Asp 1246 in Pgh1. In this manner, we generated (1) the parasite line D10-mdr^{D10} which retained the wild-type *pfmdr1* sequence, (2) the parasite line D10-mdr$^{7G8/3}$ into which the *pfmdr1* gene encoding the Cys 1034, Asp 1042 and Tyr 1246 mutations was inserted, and (3) the parasite line D10-mdr$^{7G8/1}$ which encoded the Tyr 1246 mutation in *pfmdr1* owing to a single recombination event in the gene between the codons encoding this amino acid and position 1042 (Fig. 1a). Analysis of genomic DNA by Southern hybridization (Fig. 1b) and sequencing of the *pfmdr1* gene confirmed these integration events.

To determine the role of the Cys 1034, Asp 1042 and Tyr 1246 substitutions in a distinct genetic background, we made similar constructs for CQR 7G8 parasites and carried out analogous experiments. Plasmid pHH1-mdr^{D10} (Fig. 1c) allowed allelic replacement of the *pfmdr1* gene within 7G8 parasites such that the gene encoded the wild-type (D10) amino acids Ser 1034, Asn 1042 and Asp 1246. The two cloned lines, 7G8-mdr$^{D10/c1}$ and 7G8-mdr$^{D10/c2}$, were generated in this manner (Fig. 1c). pHH1-mdr^{7G8} (Fig. 1c) served as a transfection control and, once integrated, retained the mutant *pfmdr1* allele (7G8-mdr^{7G8} parasites; Fig. 1c).

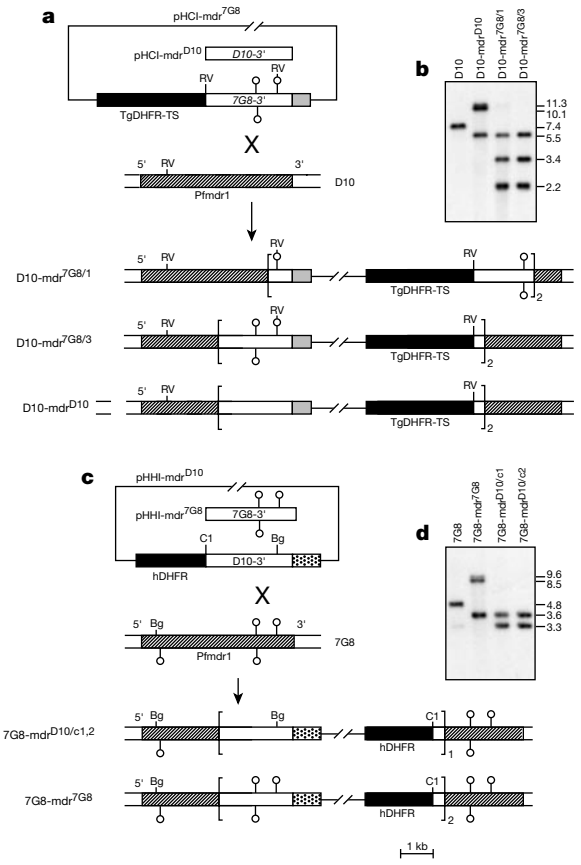

Figure 1 Allelic replacement of the *pfmdr1* gene. **a**, Allelic replacement of the *pfmdr1* gene in the D10 cloned parasite line. The transfection plasmids pHC1-mdr^{7G8} and pHC1-mdr^{D10} are shown. Open circles indicate the mutations Cys 1034, Asp 1042 and Tyr 1246 in pHC1-mdr^{7G8} (ref. 1). The codon for Tyr 1246 creates an *Eco*RV site that was used to map the integration events for this plasmid. The selection cassette Tg*dhfr-ts* (*Toxoplasma gondii* dihydrofolate reductase-thymidylate synthase), which confers resistance to pyrimethamine[20–22] is indicated. The integration structure for D10-mdr$^{7G8/1}$, in which the recombination event occurred between the Asp 1042 and Tyr 1246 polymorphisms in the pHC1-mdr^{7G8}plasmid resulting in the introduction of only the Tyr 1246 mutation in the endogenous *pfmdr1* gene, and the structures of the plasmid integration events in D10-mdr$^{7G8/3}$ (for plasmid pHC1-mdr ^{7G8}) and D10-mdr^{D10} (for plasmid pHC1-mdr^{D10}) are shown. All integration events occurred through a single recombination event resulting in reconstitution of the *pfmdr1* gene and displacement of a fragment of the gene downstream with insertion of two copies of the plasmid in each case[8]. RV, *Eco*RV. **b**, Southern hybridization of genomic DNA digested with *Eco*RV from each parasite line. **c**, Allelic replacement of the *pfmdr1* gene in the 7G8 cloned parasite line. The transfection plasmids pHH1-mdr^{D10} and pHH1-mdr^{7G8} are shown. The selection cassette includes the human *dhfr* gene. Integration events are shown for the two clones 7G8-mdr$^{D10c1/c2}$ and 7G8-mdr^{7G8}. The codon for Asp^{1246} creates a *Bgl* II site. Bg, *Bgl* II; CI, *Cla*1. **d**, Southern hybridization of *Bgl*II/*Cla*I-digested genomic DNA from each parasite line. Size of DNA fragments are shown in kb (**b**,**d**).